Short communication

# Electrochemical properties of LiMnO$_2$ for lithium polymer battery

En Mei Jin[a], Bo Jin[b,a], Yeon-Su Jeon[a], Kyung-Hee Park[a], Hal-Bon Gu[a,*]

[a] Department of Electrical Engineering, Chonnam National University, 300 Yongbong-dong, Buk-gu, Gwangju 500-757, Republic of Korea
[b] College of Materials Science and Engineering, Jilin University, Changchun 130025, China

ABSTRACT

Well-defined o-LiMnO$_2$ cathode materials were synthesized by quenching method at 1050 °C in an argon flow. The synthesized LiMnO$_2$ particle was characterized by X-ray diffraction (XRD) and field emission scanning electron microscopy (FE-SEM). LiMnO$_2$/solid polymer electrolyte (SPE)/Li batteries were characterized electrochemically by charge/discharge experiments, cyclic voltammetry (CV) and ac impedance spectroscopy. The charge/discharge results show that the discharge capacities of LiMnO$_2$ are 62 mAh g$^{-1}$ at the first cycle and 124 mAh g$^{-1}$ after 70 cycles, respectively. Moreover, we evaluated batteries using liquid electrolyte and SPE. From the charge/discharge results, the discharge capacity of LiMnO$_2$/SPE/Li battery is greater than that of LiMnO$_2$/Li battery with liquid electrolyte.

© 2008 Published by Elsevier B.V.

## 1. Introduction

Lithium polymer batteries have been utilized in a wide range of applications, such as cellular phones, notebooks, camcorders and digital cameras [1,2]. The successful commercialization of Li-ion gel polymer batteries for portable electronic devices has led to the other applications where the size and weight of batteries are important. A considerable investment in this battery technology that utilizes LiCoO$_2$ cathodes has been made [3–8]. However, low-cost cathode materials are required for many applications such as in electrical vehicles (EVs) and hybrid electric vehicles (HEVs) [9,10]. The Mn-based materials have attracted attention as intercalation cathode materials because of their low cost and nontoxicity. The LiMn$_2$O$_4$ has shown excellent cycle performance at room temperature in the 4 V region, but also exhibits a significant capacity loss in the 3–4 V region as well as at high-temperature [11,12]. In contrast to LiMn$_2$O$_4$, the trivalent manganese compounds LiMnO$_2$ (both orthorhombic and monoclinic) exhibited a better cyclability even between 2 and 4.5 V vs. Li$^+$/Li [13,14]. Orthorhombic LiMnO$_2$ (hereafter referred to as o-LiMnO$_2$) should be the best substitute for spinel LiMn$_2$O$_4$. Meanwhile, it becomes clear that o-LiMnO$_2$ is particularly attractive because of its potential to offer a high theoretical capacity of 286 mAh g$^{-1}$, which is twice that of spinel LiMn$_2$O$_4$ within the same Mn$^{4+}$/Mn$^{3+}$ redox couple [15,16]. Orthorhombic LiMnO$_2$ can be synthesized by various methods such as

solid-state method [4], hydrothermal method [17] and quenching method [18].

In this study, o-LiMnO$_2$ particles were prepared by quenching method. The electrochemical properties of the as-synthesized o-LiMnO$_2$ for lithium ion batteries and lithium polymer batteries are presented.

## 2. Experimental

Orthorhombic LiMnO$_2$ was prepared with the starting materials of LiOH·H$_2$O (Aldrich, 99.995%) and Mn$_3$O$_4$ (Aldrich, 97%) by quenching method. The precursors were mixed. After the mixture was pelleted and heated at 1050 °C for 15 h, the obtained sample was cooled by liquid state of nitrogen. The heating rate was 10 °C min$^{-1}$. The resulting LiMnO$_2$ was obtained after ball-milling at 300 rpm for 10 h.

The crystalline phases of the obtained o-LiMnO$_2$ powders were identified with X-ray diffraction (XRD, Dmax/1200, Rigaku). The XRD pattern was collected by a step-scanning mode in the range of 10–80° with a step time of 5° min$^{-1}$. Powder morphologies were observed by FE-SEM.

The composite electrodes were prepared by mixing o-LiMnO$_2$, acetylene black (AB) and polyvinylidenefluoride (PVDF) binder dissolved in N-mehtylpyrrolidinone in different weight ratios. The obtained slurry was ball-milled for 1 h, and coated onto an Al-foil, and dried at 90 °C for 1 h. The resulting electrode films were pressed with a twin roller, cut into a round plate ($\Phi$ = 15.958 mm), and dried at 110 °C for 24 h under vacuum. A lithium foil was used as an anode. Liquid electrolyte was 1 M LiPF$_6$ dissolved in ethy-

lene carbonate (EC)/dimethyl carbonate (DMC) (EC:DMC = 1:1). 25PVDFLiClO$_4$ EC$_{10}$PC$_{10}$ was used as SPE and its synthesis was described in detail previously [19]. The coin-type cells (CR2032) were fabricated for the electrochemical tests. LiMnO$_2$/SPE/Li batteries and LiMnO$_2$/Li batteries were fabricated in an argon-filled glove box. The charge/discharge testing was performed using automatic charge/discharge equipment (WBCS3000, WonATech Co.) in a potential range of 2.0–4.3 V at a constant current density of 0.2 mA cm$^{-2}$ at 25 °C.

Electrochemical impedance measurements were performed using an IM6 impedance system (Zahner Elektrik Co.). The spectrum was potentiostatically measured by applying an ac voltage of 10 mV over the frequency range from 10 to 1 MHz. The WBCS3000 (WonATech Co.) Battery Tester System was also used for the measurements of cyclic voltammetry in a potential range of 2.0–4.3 V at a scan rate of 0.1 mV s$^{-1}$.

## 3. Results and discussion

### 3.1. Crystal structure

The XRD pattern of o-LiMnO$_2$ powders is shown in Fig. 1. The XRD pattern of the compound o-LiMnO$_2$ can be indexed to a single-phase material having an orthorhombic structure, which is the same as the works of Myung et al. [20].

### 3.2. Morphology analysis

The FE-SEM image of o-LiMnO$_2$ powders is shown in Fig. 2. As can be seen from Fig. 2, the average particle size of o-LiMnO$_2$ powders is around 1.5 μm in the length and 0.5 μm in the width. The morphology of o-LiMnO$_2$ is bar-type, which is the typical crystallite pattern [21,22].

### 3.3. Charge/discharge properties

The cycling performance of LiMnO$_2$/SPE/Li batteries with different electrode combination ratios (LiMnO$_2$:AB:PVDF = 85:10:5, 80:15:5 and 75:20:5) is shown in Fig. 3. The batteries were cycled between 2.0 and 4.3 V at a current density of 0.2 mA cm$^{-2}$. As can be seen from Fig. 3, the initial discharge capacities of LiMnO$_2$/SPE/Li batteries with electrode combination ratio of 75:20:5, 80:15:5 and
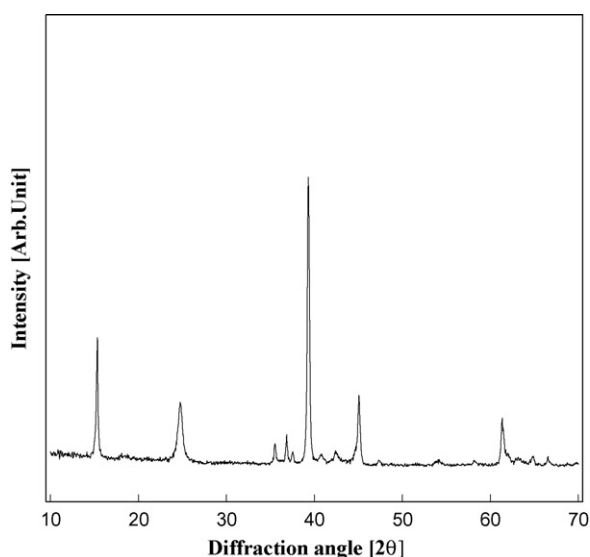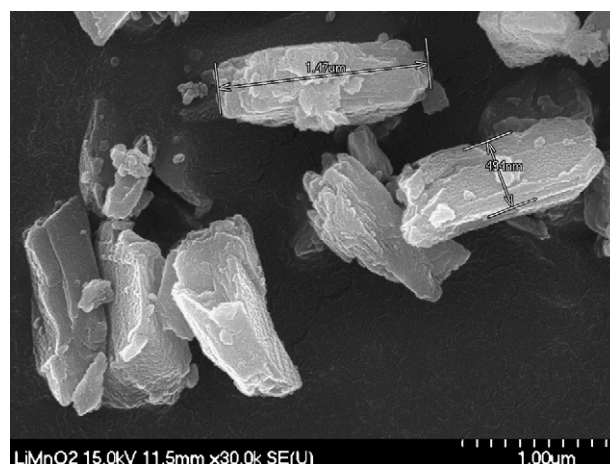
**Fig. 2.** The FE-SEM image of prepared o-LiMnO$_2$ powders by quenching method.

85:10:5 are 52, 62 and 54 mAh g$^{-1}$, respectively. The maximum discharge capacities are 76, 124 and 104 mAh g$^{-1}$ at the 40th, 50th and 60th cycle, respectively. It is demonstrated that the cycling performance of LiMnO$_2$/SPE/Li cell with electrode combination ratio of 80:15:5 is better than that of other batteries. Moreover, we evaluated liquid electrolyte and solid polymer electrolyte. Fig. 4 shows the cycling performance of LiMnO$_2$/SPE/Li battery and LiMnO$_2$/Li battery with liquid electrolyte with electrode combination ratio of 80:15:5. As can be seen from Fig. 4, the discharge capacities of LiMnO$_2$/SPE/Li battery are 62 mAh g$^{-1}$ at the first cycle and 124 mAh g$^{-1}$ after 70 cycles, respectively. The cycling performance of LiMnO$_2$/SPE/Li battery is better than that of LiMnO$_2$/Li battery with liquid electrolyte.

### 3.4. Cyclic voltammetry

The obtained o-LiMnO$_2$ sample heated at 1050 °C was examined by cyclic voltammetry. The LiMnO$_2$/SPE/Li battery was tested between 2.0 and 4.3 V at a scanning rate of 0.1 mV s$^{-1}$. The cyclic voltammetry can also be used to reveal the reactions occuring during the transformation. Fig. 5 shows the cyclic voltammograms. As
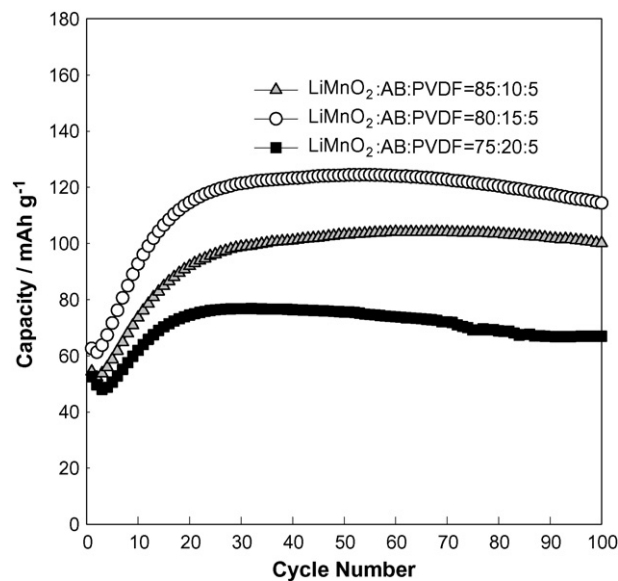
**Fig. 1.** The XRD pattern of the o-LiMnO$_2$ powders.

**Fig. 3.** The cycling performance of LiMnO$_2$/SPE/Li batteries with different electrode combination ratios.
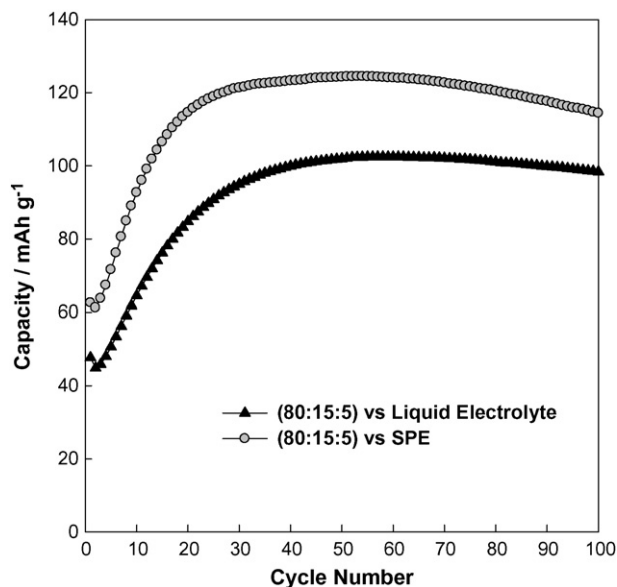
**Fig. 4.** The cycling performance of LiMnO$_2$/Li battery with liquid electrolyte and LiMnO$_2$/SPE/Li battery with electrode combination ratio of 80:15:5.



**Fig. 6.** The ac impedance spectra of LiMnO$_2$/SPE/Li upon cycling.

shown from Fig. 5, there are one distinct oxidation peak at 3.2 V, and three small reduction peaks around at 4.0 V. The characteristic redox peaks of spinel LiMn$_2$O$_4$ at around 3.95 and 4.10 V are observed in the plot. The height of the redox peaks around 3.1 and 4 V increase with cycling, indicating a progressive formation of cycle induced spinel phase, and become saturated after cycles [23]. These results are in consistent with those shown in Fig. 4, though capacity saturation is found at higher cycle number than that obtained from capacity retention study.

### 3.5. Impedance properties

Impedance spectra of LiMnO$_2$/SPE/Li upon cycling are shown in Fig. 6. It is noted that the ac impedance response of the cell forms a broad semicircle and a line to the real axis in the lowest frequency range. The semicircle in the high frequency is mainly related to
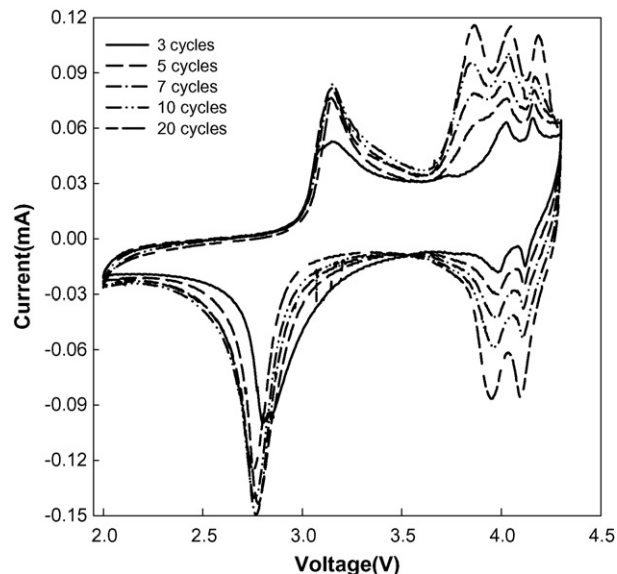
the complex reaction process at the electrolyte/cathode interface including resistance of SEI film formed on the surface o-LiMnO$_2$ particles, the particle-to-particle contact resistance, charge transfer resistance, and corresponding capacitances. The inclined line in the lower frequency is attributed to the Warburg impedance, which is associated with lithium-ion diffusion in o-LiMnO$_2$ electrode. As can be seen from Fig. 6, the resistances are 150 Ω at the first cycle, 120 Ω after 2 cycles, 110 Ω after 10 cycles, respectively. It is obvious that LiMnO$_2$/SPE/Li battery resistance slacks up upon cycling. This result is consistent with the cycling performance of LiMnO$_2$/SPE/Li battery with electrode combination ratio of 80:15:5 (as shown in Fig. 4).

### 4. Conclusions

Orthorhombic LiMnO$_2$ cathode materials were prepared by quenching reaction. The prepared o-LiMnO$_2$ can be indexed to a single-phase material having the orthorhombic structure. Among LiMnO$_2$/SPE/Li batteries with different electrode combination ratios (LiMnO$_2$:AB:PVDF = 85:10:5, 80:15:5 and 75:20:5), LiMnO$_2$/SPE/Li battery with electrode combination ratio of 80:15:5 is the best. The cycling performance of LiMnO$_2$/SPE/Li battery is better than that of LiMnO$_2$/Li battery with liquid electrolyte. The initial discharge capacity of LiMnO$_2$/SPE/Li battery is 62 mAh g$^{-1}$ and the maximum discharge capacity is 124 mAh g$^{-1}$ at the 70th cycle.

### Acknowledgment

### References

[1] Q. Liu, D. Mao, C. Chang, F. Huang, J. Power Sources 173 (2007) 707.
[2] S. Wu, M. Yu, J. Power Sources 165 (2007) 660.
[3] P. Suresh, A.K. Shukla, N. Munichandraiah, J. Power Sources 161 (2006) 1307.
[4] Y.J. Wei, H. Ehrenberg, N.N. Bramnik, K. Nikolowski, C. Baehtz, H. Fuess, Solid State Ionics 178 (2007) 253.
[5] G. Fan, Y. Zeng, R. Chen, G. Lü, J. Alloys Compd. 461 (2008) 267.
[6] P. Ghosh, S. Mahanty, R.N. Basu, Mater. Chem. Phys. 110 (2008) 406.
[7] M. Park, S. Hyun, S. Nam, S. Cho, Electrochim. Acta 53 (2008) 5523.

**Fig. 5.** The cyclic voltammetry of LiMnO$_2$/SPE/Li in a potential range of 2.0 and 4.3 V at a scanning rate of 0.1 mV s$^{-1}$ at 25 °C.
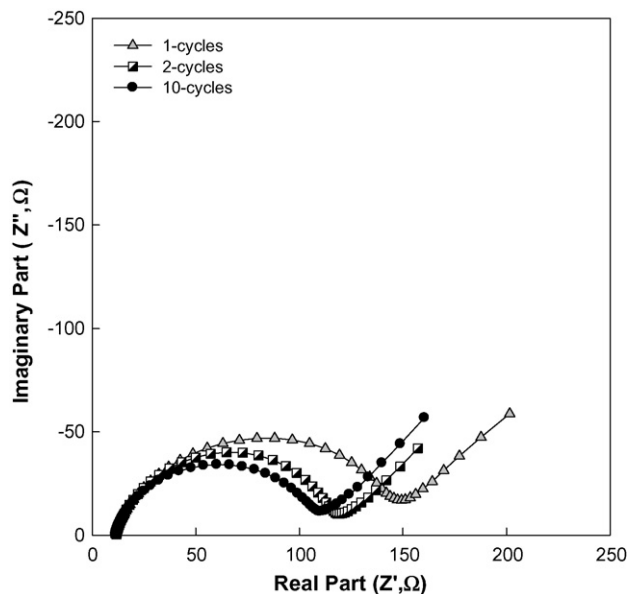
[8] S. Vivekanandhan, M. Venkateswarlu, N. Satya-narayana, Mater. Chem. Phys. 109 (2008) 241.

[9] M. Wu, Q. Zhang, H. Lu, A. Chen, Solid State Ionics 169 (2004) 47.

[10] C. Li, H.P. Zhang, L.J. Fu, H. Liu, Y.P. Wu, E. Rahm, R. Holze, H.Q. Wu, Electrochim. Acta 51 (2006) 3872.

[11] J.M. Jarscon, E. Wang, F.K. Shokoohi, J. Electrochem. Soc. 138 (1991) 2859.

[12] J. Barker, R. Koksbang, M.Y. Saidi, Solid State Ionics 82 (1995) 143.

[13] R.J. Gummow, D.C. Liles, M.M. Thackeray, Mater. Res. Bull. 28 (1993) 1249.

[14] A.R. Armstrong, P.G. Bruce, Nature 381 (1996) 499.

[15] P.G. Bruce, Chem. Commun. (1997) 1817.

[16] M.M. Thackeray, Prog. Solid State Chem. 25 (1997) 1.

[17] F. Zhou, X. Zhao, Y. Liu, L. Li, C. Yuan, J. Phys. Chem. Solids 69 (8) (2008 2061).

[18] Y.S. Lee, Y.K. Sun, K. Adachi, M. Yoshio, Electrochim. Acta 48 (2003) 1031.

[19] J.-U. Kim, Y.-J. Jo, G.-C. Park, W.-J. Jeong, H.-B. Gu, J. Power Sources 97–98 (2001) 450.

[20] S.T. Myung, S. Komaba, K. Kurihara, N. Kumagai, Solid State Ionics 177 (2006) 733.

[21] M. Yoshio, H. Noguchi, T. Miyashita, H. Nakamura, A. Kozawa, J. Power Sources 54 (1995) 483.

[22] Y.S. Lee, C.S. Yoon, Y.K. Sun, M. Yoshio, Electrochem. Solid-State Lett. 5 (1) (2002) A1.

[23] S.-H. Wu, M.-T. Yu, J. Power Sources 165 (2007) 660.